Turbulence effects on bi-directional ground-to-satellite laser communication systems

Nicolas Védrenne,
Marie-Thérèse Velluet,
Marc Séchaud,
Jean-Marc Conan
ONERA,The French Aerospace Lab,
92320 Châtillon, France
Email: nicolas.vedrenne@onera.fr

Morio Toyoshima,
Hideki Takenada
NICT
4-2-1 Nukui-Kitamachi,
Koganei, Tokyo 184-8795, Japan

Alexandre Guérin,
Frédéric Lacoste
CNES
18 Avenue Edouard Belin,
31401 Toulouse Cedex 9, France

***Abstract*—Satellite-to-ground communications are currently facing new challenges in terms of data rates. With expected data rates as high as tens of Gbps, optical technologies should contribute to solve the issue. Unfortunately turbulence can severely jeopardize optical communication performance. So as to evaluate the impact of turbulence on data rates and on optical system design, an end-to-end code, based on phase screen techniques, has been adapted to simulate the propagation channel in LEO-Ground configurations. Compared to analytical expressions, our code allows to simulate strong scintillations, joint pointing and turbulence effects, and derivation of spatial and temporal statistics. We illustrate the use of this tool by modeling flux fluctuations in a telescope receiver for up and down link between LEO satellite and an optical ground station. For down-link, the access to the experimental optical data recorded by NICT ground station of OICETS satellite allows to discuss the simulated results in view of the development of the future ground to space optical links.**

I. Introduction

In the space domain, laser communications can face the demand of the future Earth Observation missions by offering significant improvements compared to classical radio-frequency communications: increased data rates with reduced power consumption, mass and size [1].

Laser beam propagation through the atmosphere can be significantly impaired by atmospheric turbulence. To limit the influence of these perturbations on communication performance, dedicated communications protocols must be designed. To adapt their parameters to the specificities of the perturbations, statistical properties of the perturbations must be accurately known. Analytical models exist to describe turbulence effect on laser beam propagation. However their accuracy is usually limited to the small perturbations approximation[2], [3], [4]. For stronger perturbations, which is usually the case for low elevation line of sights, heuristic models have been developed, but their use is restricted to very specific cases[5]. To model beam propagation through atmospheric turbulence, numerical models of the propagation channel have been developed, based on phase screen techniques[6], [7]. These tools can manage from small to very strong perturbations, they are able to consider coupled effect of pointing jitter and turbulence and they can be adapted to simulate temporal evolution. For phase screen techniques the issue is sampling (spatial and temporal) of the physical phenomena. It requires an accurate parametrization to ensure realistic results at a manageable computation cost. For more than a decade, ONERA is developing its phase screen numerical model[8]. An automatically parametrized version of this model dedicated to ground-satellite laser communications, called TURANDOT, has been delivered to CNES. It simulates the propagation channel for up-link and down-link user defined configurations. For validating TURANDOT for up-link, statistical spatial characteristics of beam irradiance profile were compared to expected beam profile[3]. In this paper we illustrate for up-link the advantages of a phase screen algorithm for system dimensioning. For down-link, TURANDOT results were compared to data presented by the National Institute of Information and Communication Technology (NICT) in [9], [10], [11]. These data were recorded on the Optical Inter-orbit Communications Engineering Test Satellite (OICETS). We present here the comparison of TURANDOT results with NICT measurements.

Section II presents TURANDOT. Section III illustrates the advantages of TURANDOT for system dimensioning in an up-link scenario. In section IV we compare TURANDOT to OICETS down-link measurements performed by NICT.

II. TURANDOT

A. TURANDOT: *the automatic* PILOT

This section is dedicated to the description of TURANDOT. TURANDOT is based on the phase screen algorithm of ONERA, called PILOT (Propagation and Imaging, Laser and Optics, through Turbulence). PILOT is dedicated to study situations which cannot be described satisfactorily with analytical approaches such as the so-called scintillation saturation regime, temporal evolution, anisoplanatism and laser beam propagation. It is able to consider all type of wave-forms (spherical, plane or truncated Gaussian beams), to deal with high turbulence strength and extended objects (anisoplanatism effects[12], [13], [14]). It is as well able to simulate temporal evolution of the perturbations. For what concerns space communication systems, it deals with very low elevation angles,

temporal statistics, point-ahead angle and laser beam propagation. Besides, this simulation tool allows the joint account of pointing and turbulence effects, emission wavefront quality and the joint derivation of spatial and temporal statistics. It has been used in the Astrium LOLA project ([15]) to study the propagation channel and in the HPFDIS study leaded by ESA to quantify the effect of atmospheric turbulence on long range optical link with heterodyne detection and correction. PILOT has been used to design numerous adaptive optics (AO) systems for telecoms, laser focusing and space observation ([16], [17], [18], [14], [19], [20]). It has been extensively compared to analytical formulas [13], [14], [21] and to experimental data for different applications.

In order to manage the simulation parameters issue, ONERA has developed dimensioning tools to optimize the computation time while ensuring reliable simulation results with PILOT. For ground-LEO laser communications ONERA has associated its phase screen dimensioning tool dedicated to laser communications with PILOT to deliver TURANDOT, the automatically parametrized PILOT version.

B. Inputs/outputs

The parameters of the simulation are derived from a user defined communication scenario. User defined scenario corresponds to the definition of:

- the direction of the propagation: up-link or down-link;
- the parameters of the satellite (elevation θ, transverse velocity v_{sat}, the distance ground-satellite);
- the parameters of the transceivers: the emission and reception diameters, the geometry of the transceivers, their optical quality, pointing jitter;
- the parameters of the beam: wavelength and beam divergence at emission;
- the parameters of the atmosphere: the transverse wind velocity v_{wind}, the C_n^2 profile or the C_n^2 value at ground level and the stability of the atmosphere depending whether a user defined C_n^2 profile has been provided or not.

Temporal horizon and the number of samples are user-defined inputs. User defined C_n^2 profile, aberrated wavefront map at emission and temporal series of pointing jitter can also be loaded.

From these physical parameters, TURANDOT is able to compute automatically the phase screen parameters: width, spatial sampling, position along the line of sight. Parameters are optimized to ensure a reasonable simulation duration. A typical temporal simulation (1 s temporal serie at 10 kHz sampling) takes 1 hour on dedicated workstation.

The outputs of TURANDOT are the instantaneous propagated field (amplitude and phase) in the receiver aperture and several parameters relevant to turbulence influence on beam propagation, like angle of arrival standard deviation for instance. From the instantaneous propagated field, collected flux in the receiver aperture and focal plane irradiance distribution can be directly derived. The knowledge of flux fluctuations variance, power spectral density and probability density function allows to estimate communication performances and to adapt and optimize signal coding. The robustness of corrector error codes to the strong variability of the C_n^2 profile can be extensively investigated and corrector error codes parameters tuned consequently.

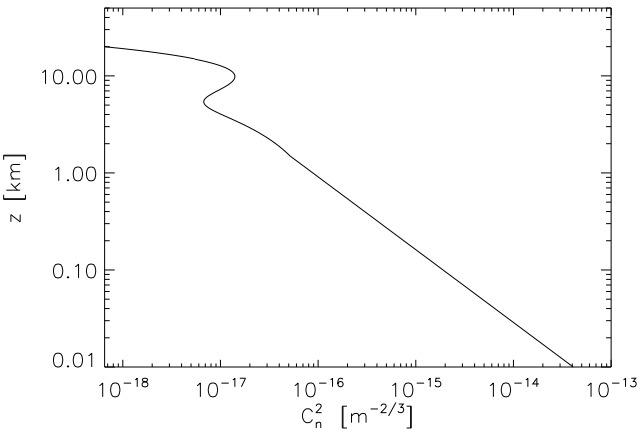

Fig. 1: Vertical C_n^2 profile used for the up-link scenario.

III. UP-LINK

We present here TURANDOT results for an up-link propagation scenario. The aim is to illustrate turbulence influence on the characteristics of the flux collected by a LEO satellite in the case of a small divergence beam (2.5 μrad).

For this scenario the Gaussian beam waist is located in the pupil of the emitter, the amplitude beam radius at 1/e is set to w_0 = 0.1 m. The propagation wavelength is λ = 847 nm, the distance ground-satellite is d_{sat} = 800 km, the satellite transverse velocity is v_{sat} = 8 km/s, satellite elevation is θ = 20°, receiver aperture diameter is D_{sat} = 0.3 m. With these parameters a diffraction limited beam would have a 1/e diameter in amplitude of approximately 2.1 m in the receiver plane. No pointing jitter is considered here, in order to focus on turbulence effects.

TURANDOT enables to take into account the effect of a natural wind which is added to the screens displacement caused by the satellite movement. In the up-link case, an homogeneous wind profile with a transverse velocity $v_{wind} = 10$ m/s is assumed. The vertical C_n^2 profile used for the simulation is presented in figure 1. For high altitude layers, it corresponds to a Hufnagel-Valley profile [22], for low altitude layers C_n^2 decreases against altitude with a similitude power law in $h^{-4/3}$. This power law is typical of a day-time atmosphere above a rural area[23], [24]. The turbulence profile is chosen to ensure a C_n^2 =2 10^{-13} $m^{-2/3}$ at ground level. The Fried diameter for a plane wave computed along the path is r_0 =10 cm. Time sampling is performed at 20 kHz, 1000 samples are simulated. The simulation takes less than 4 minutes on a dedicated workstation.

Evolution of the flux collected in the receiver aperture normalized to the emitted flux on a duration of 50 milliseconds is

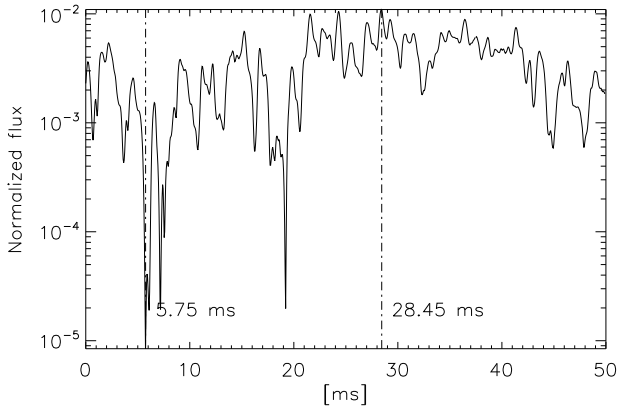

Fig. 2: Collected flux in the receiver aperture normalized to the emitted flux on a 50 ms duration.

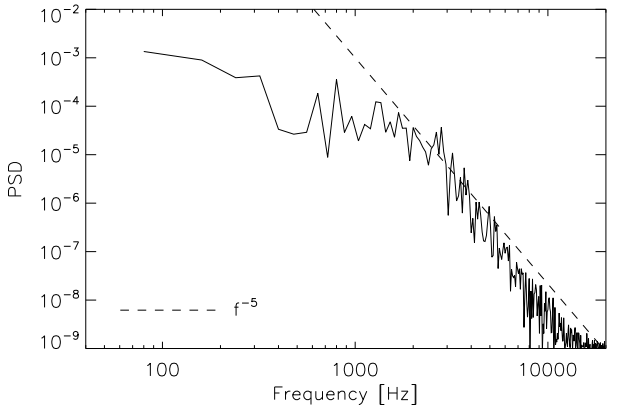

Fig. 3: Temporal power spectral density of the flux collected by the receiver aperture for a 50 ms duration.

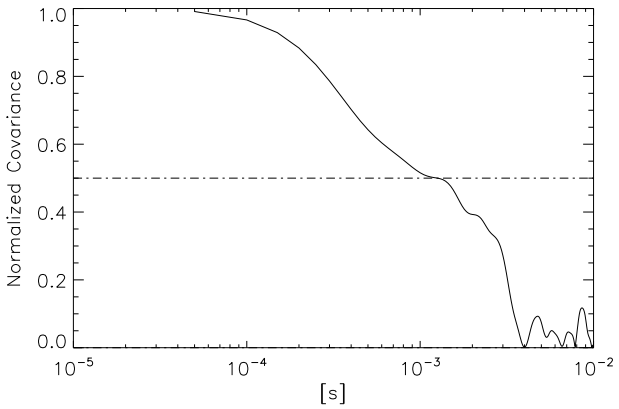

Fig. 4: Normalized temporal correlation of the flux collected by the receiver aperture on a 50 ms duration.

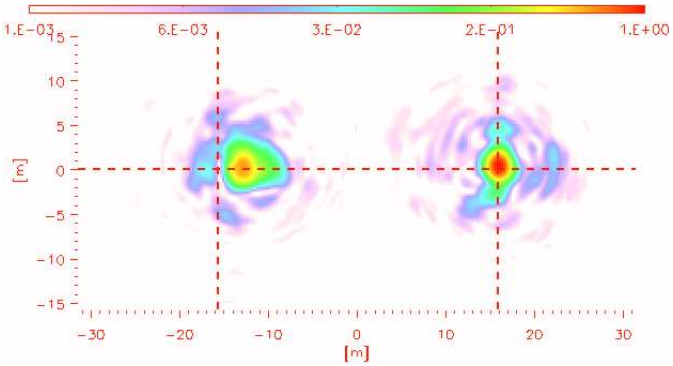

Fig. 5: Intensity beam profile in receiver plane at two instants. The horizontal size of the image corresponds to 64 m. The cross indicates the satellite position.

presented in figure 2. The average flux is approximately 0.002. It theoretically corresponds to the ratio of the aperture surface ($\pi D_{sat}^2/4$) on the size of the turbulence induced diffraction pattern $\lambda d_{sat}/r_0$. We find here $\pi D_{sat}^2/4/(\lambda d_{sat}/r_0) = 1.5\ 10^{-3}$. The difference can be explained by numerical convergence. The figure clearly shows how strong can be the variations of the flux caused by atmospheric turbulence. The normalized flux fluctuations variance is 0.4.

Temporal power spectral density of flux fluctuations is plotted in figure 3. Analysis of the figure enables the identification of a power law for high temporal frequencies close to f^{-5}. This is consistent with the $f^{-14/3}$ expected power law according to [25], [26].

Normalized temporal correlation of the flux is presented in figure 4. Normalized temporal correlation drops below 0.5 for the temporal correlation time T_c = 1 ms.

Results presented here illustrate the impact of turbulence on flux fluctuations in the case of a small divergence Gaussian beam. In this case, the beam radius at emission and the Fried diameter are very close. Turbulence effects on the beam profile mostly consist in a beam wander, the strong flux variations in the receiver are therefore mainly due to the beam movement. This is confirmed by the analysis of the beam intensity profile in the receiver plane, showed in figure 5. On the left the beam position corresponds to the minimum of collected flux (see figure 2, T = 5.75 ms). On the right the beam position corresponds to the maximum of the collected flux (see figure 2, T = 28.45 ms). Colorscale is logarithmic. The intersections of the dotted lines correspond to the optical axis (theoretical receiver position). The receiver aperture size (30 cm) is small compared to that of intensity structures. The maximum flux corresponds to a beam centered on the satellite location. The minimum flux results from a displacement of the beam larger than the beam radius. We illustrate here the influence of beam wander on flux fluctuations. According to TURANDOT, the standard deviation of angle of arrival, computed from the beam displacement in receiver plane, is 3 µrad. So, pointing jitters smaller than this should ensure a system design limited by turbulence effects and not by pointing errors.

We illustrate here the interest of TURANDOT. It gives access to temporal varying series (several seconds) of collected flux. Data analysis of the temporal series delivers information

Elevation	Distance [km]	Velocity [km/s]	σ_χ^2	r_0 [m]
23.5°	1262	5.9	0.12	0.06
35.1°	963	7.5	0.07	0.07

Fig. 6: Parameters of TURANDOT in the down-link scenario. σ_χ^2 and r_0 are computed from the C_n^2 profile along the line of sight.

for dimensioning laser communication systems, the temporal correlation length gives for example access to the burst error duration. This is crucial to determine the adequate packet size and coding length of the signal. Furthermore, turbulence effects and pointing errors are simultaneously taken into account on the propagated field and consequently on the signal. For the small divergence case considered here, turbulence effect mostly consists in a beam wander. Pointing jitter should be kept smaller than 3 µrad for being neglected.

IV. Down-link

A. OICETS- NICT *experiment*

TURANDOT results are now compared with experimental measurements of NICT optical ground station. Data were collected during bi-directional ground-satellite laser communication experiments performed between October 2008 and January 2009[9], [10], [11]. During these experiments the flux emitted by the Laser Utilizing Communications Equipment (LUCE) aboard OICETS have been recorded on a pin-photo diode with a 5 cm aperture. The sampling frequency of the flux measurement was 20 kHz. Various satellite elevations were considered. We focus here on data gathered during the night of December 23, 2008 and selected two elevations : 23.5 ° and 35.1 °.

B. *Simulation*

The parameters of the experiment relevant to the numerical simulation are reported in table 6. Transverse velocities of the satellite are deduced from antenna slew rate presented in figure 5 of [27]. The laser wavelength is 847 nm and beam diameter of the receiver on OICETS is 12 cm.

The vertical C_n^2 profile is chosen to be representative of experimental conditions. As the line of sight is mostly above an urban area, a Hufnagel-Valley C_n^2 profile with a $h^{-4/3}$ power law for low altitude layers is chosen. The ground level C_n^2 is set to ensure a plane wave Fried diameter [28] of r_0 = 7 cm (@λ = 847 nm) for θ = 35.1°. This leads to C_n^2 = 3.5 10^{-14} $m^{-2/3}$ at ground level. Log-amplitude variance, denoted σ_χ^2, computed using the C_n^2 profile projected along the line of sight and the usual analytical formula for plane wave taken from [2] are reported in table 6. The Fried diameter for each elevation is also reported in table 6. We assume an identical vertical profile in both cases. This might not be the case during the experiment, because of the difference of elevation.

Temporal series of collected flux in the receiver aperture are simulated for the two elevations. Total duration of a temporal serie is 80 ms, simulation sampling frequency is 20 kHz. The simulation of the 1600 time samples for one elevation takes 10 minutes on a workstation.

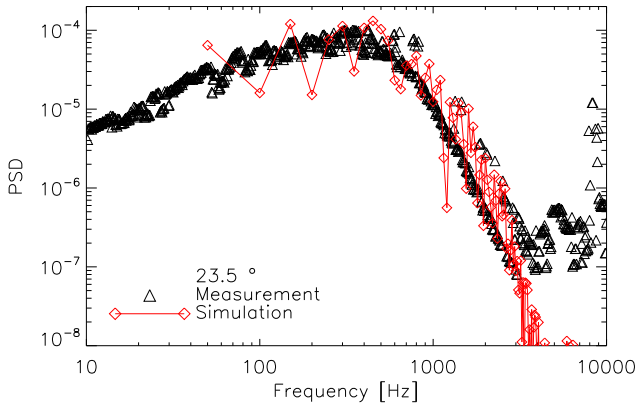

Fig. 7: Power spectral density of the collected flux, 23,5° measurements (black △), simulation results (red ⋄, continuous line).

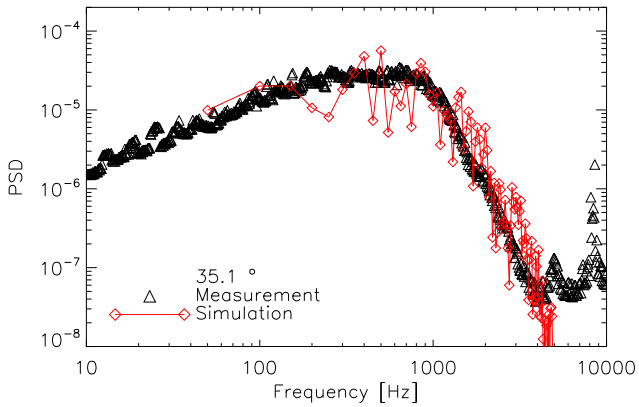

Fig. 8: Power spectral density of the collected flux, 35,1° measurements (black △), simulation results (red ⋄, continuous line).

C. *Experimental and simulated data analysis*

Statistical characteristics are derived here from the analysis of simulated data. Power spectral densities (PSD) of the measurements reported in [27] are compared to PSD computed from the temporal series simulated with TURANDOT. Measured PSD are plotted in black △ in figure 7 for θ =23.5° and in figure 8 for θ =35.1°. Numerical simulation results are plotted in red ⋄ and continuous line. A significant agreement between numerical simulation and experimental results is demonstrated for both elevations. The global trend of the experimental PSD is well fitted by the numerical one, cut-off frequencies and asymptotic trends are observed in both cases.

Measured normalized temporal correlation are plotted in

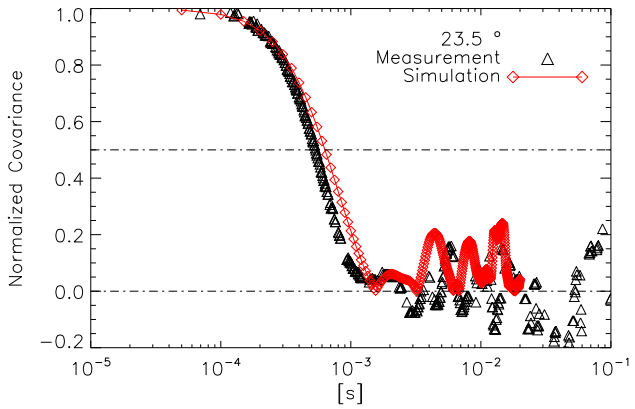

Fig. 9: Normalized temporal correlation, 23,5° measurements (black △), simulation results (red ◇, continuous line).

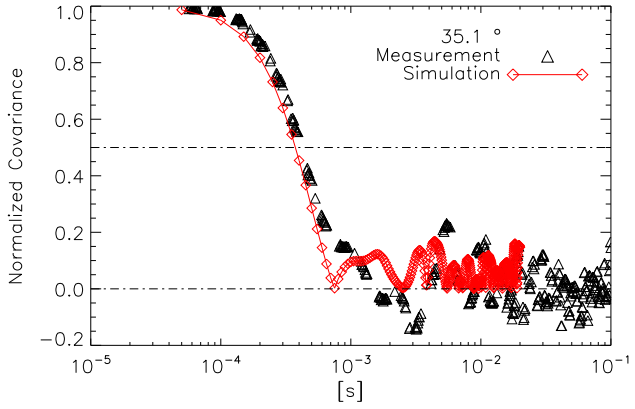

Fig. 10: Normalized temporal correlation, 35,1° measurements (black △), simulation results (red ◇, continuous line).

black △ in figure 9 for θ =23.5° and on figure 10 for θ =35.1°. Numerical simulation results are plotted in red ◇ and continuous line.

Analysis of the normalized temporal correlation enables to evaluate the correlation time T_c. It corresponds to the duration where the temporal correlation drops below 0.5. Correlation time is reported in table 11 for the two elevations.

For θ =35.1°, the difference between measurements and numerical results is 5%, which is very good. The precision is worse for θ = 23.5°. The largest uncertainty comes from the C_n^2 and wind profiles chosen for simulation. Considering the precision of temporal correlation it appears that the assumption

Elevation	Measured [µs]	Simulated [µs]
23.5°	500	600
35.1°	400	380

Fig. 11: Temporal correlation T_c for both elevations, obtained from measurements (left) and from simulation results (right).

we made on these two profiles seems more justified for θ =35.1° than for θ =23.5°.

According to table 11, T_c increases when the elevation decreases. This can be explained physically with a very simple single layer description. Let us consider that the main contribution to the scintillation phenomena comes from a single turbulent layer located at a distance z from the receiver for elevation θ. Phase perturbations due to this layer cause in the receiver plane speckle patterns with typical size $\sqrt{\lambda z}$. The temporal correlation of speckle patterns movements is proportional to the time needed for a speckle pattern to cross the aperture, that is:

$$T_c(\theta) \propto \frac{\sqrt{\lambda z(\theta)}}{\omega(\theta) z(\theta)} \tag{1}$$

where $\omega(\theta)$ is the transverse angular velocity of the satellite at elevation θ. With this single layer description the influence of wind velocity can be neglected in first approximation. Assuming the turbulence layer altitude (distance from ground) does not depend on elevation, its position along the line of sight for two elevations θ and θ' must satisfy $z(\theta) = z(\theta') \sin\theta' / \sin\theta$. This enables to relate $T_c(\theta)$ and $T_c(\theta')$ according to:

$$T_c(\theta') = T_c(\theta) \frac{\omega(\theta)}{\omega(\theta')} \left(\frac{\sin\theta'}{\sin\theta} \right)^{1/2}. \tag{2}$$

We find for the measurements $T_c(\theta' = 23.5°) = 550\,\mu s$ to be compared with 500 µs, and for the simulated results $T_c(\theta' = 23.5°) = 527\,\mu s$ to be compared with 600 µs. The single layer description enables to explain the most important part of the decorrelation. The remaining differences can be due to other layers, particularly to the low altitude ones whose effect must be taken into account especially for low elevations, because of their high C_n^2.

The C_n^2 profile appears here a key parameter of the representativeness of the simulations. The difficulty is to be able to measure it simultaneously to data acquisition. A solution could be to exploit scintillation pattern power spectral density in a large enough receiver aperture [29], [30]. Another could be to use a dedicated instrument[21], [31].

V. Conclusion

TURANDOT is a numerical tool developed at ONERA to simulate turbulence induced flux fluctuations for ground to satellite laser communication systems. The ability to simulate realistic temporal series of flux fluctuations will ease the dimensioning of laser communication systems. Thanks to the automatic parametrization of simulation parameters (samplings in particular) TURANDOT is user friendly. In addition to this, it makes system design optimization easier and more relevant because a wide panel of communications scenario can be considered. To illustrate the potential interest of TURANDOT we presented here an analysis of temporal series computed in an up-link and two down-link cases. For up-link the case of a small divergence beam has been studied. It has been shown that beam wander is the main turbulence effect. It can cause strong flux fluctuations with a typical correlation time of 1 ms.

The standard deviation of the beam angle of arrival is 3 μrad. It gives clues on the precision required for tracking. For downlink TURANDOT results have been compared to experimental measurements performed by NICT on OICETS presented in [27]. Numerical simulation and measurements agree well despite uncertainty on the C_n^2 profile and on the wind profile. More realistic results might be obtained if they were known with a better accuracy. Forthcoming experiments at low elevation (below 20°) will be performed simultaneously to C_n^2 profile measurements. To deal with these strong perturbations situations, TURANDOT code will be upgraded and exploited.

ACKNOWLEDGMENT

TURANDOT coding was supported under a Research and Technology CNES contract. The authors wish to thank Vincent Michau and Clélia Robert for fruitful discussions.

REFERENCES

[1] A. Guerin, G. Lesthievent, and J. Issler, "Evaluation of new technological concepts for high data rate payload telemetry," 2010.

[2] V. Tatarski, *Wave Propagation In a Turbulent Medium*. Dover Publications,Inc. New York, 1961.

[3] R. Fante, "Electromagnetic beam propagation in turbulent media," *Proc. of the IEEE*, vol. 63, no. 12, pp. 1669–1692, 1975.

[4] R. Sasiela, *Electromagnetic wave propagation in turbulence.* Springer-Verlag, 1994.

[5] L. Andrews and R. Phillips, *Laser Beam Propagation through Random Media*. SPIE Optical Engineering Press, Wash., 2005.

[6] R. Buckley, "Diffraction by a random phase-changing screen - A numerical experiment," *Journal of Atmospheric and Terrestrial Physics*, vol. 37, pp. 1431–1446, Nov. 1975.

[7] J. M. Martin and S. M. Flatté, "Intensity images and statistics from numerical simulation of wave propagation in 3-d random media," *Appl. Opt.*, vol. 27, no. 11, pp. 2111–2126, 1988.

[8] M. Séchaud, F. Mahé, T. Fusco, V. Michau, and J.-M. Conan, "High resolution imaging through atmospheric turbulence: link between anisoplanatism and intensity fluctuations," in *Optics in Atmospheric Propagation and Adaptive Systems V*. Florence, Italy: ESO/SPIE, Sep. 1999, pp. 243–249.

[9] M. Toyoshima, K. Takizawa, T. Kuri, W. Klaus, M. Toyoda, H. Kunimori, T. Jono, Y. Takayama, N. Kura, K. Ohinata, K. Arai, and K. Shiratama, "Ground-to-OICETS laser communication experiments," in *Society of Photo-Optical Instrumentation Engineers (SPIE) Conference Series*, ser. Society of Photo-Optical Instrumentation Engineers (SPIE) Conference Series, vol. 6304, Sep. 2006.

[10] M. Toyoshima, Y. Takayama, H. Kunimori, T. Jono, and K. Arai, "Data analysis results from the KODEN experiments," in *Society of Photo-Optical Instrumentation Engineers (SPIE) Conference Series*, ser. Society of Photo-Optical Instrumentation Engineers (SPIE) Conference Series, vol. 6709, Sep. 2007.

[11] Y. Takayama, M. Toyoshima, Y. Shoji, Y. Koyama, H. Kunimori, M. Sakaue, S. Yamakawa, Y. Tashima, and N. Kura, "Expanded laser communications demonstrations with OICETS and ground stations," in *Society of Photo-Optical Instrumentation Engineers (SPIE) Conference Series*, ser. Society of Photo-Optical Instrumentation Engineers (SPIE) Conference Series, vol. 7587, Feb. 2010.

[12] C. Robert, J. Conan, V. Michau, and T. Fusco, "Anisoplanatism in Shack-Hartmann wavefront sensing," in *Remote Sensing of Clouds and the Atmosphere IX. Proceedings of the SPIE.*, K. P. Schäfer, A. Comerón, M. R. Carleer, R. H. Picard, and N. Sifakis, Eds., vol. 5572, Nov. 2004, pp. 223–234.

[13] C. Robert, J.-M. Conan, V. Michau, T. Fusco, and N. Védrenne, "Scintillation and phase anisoplanatism in shack-hartmann wavefront sensing," *J. Opt. Soc. Am. A*, vol. 23, pp. 613–624, 2006.

[14] N. Védrenne, V. Michau, C. Robert, and J.-M. Conan, "Shack Hartmann Wavefront Estimation with Extended Sources: Anisoplanatism Influence," *J. Opt. Soc. Am. A*, vol. 24, pp. 2980–2993, Sep. 2007.

[15] V. Cazaubiel, G. Planche, V. Chorvalli, L. Le Hors, B. Roy, E. Giraud, L. Vaillon, F. Carré, and E. Decourbey, "Lola: A 40000 km optical link between an aircraft and a geostationary satellite," 2006.

[16] N. H. Schwartz, N. Védrenne, V. Michau, M.-T. Velluet, and F. Chazallet, "Mitigation of atmospheric effects by adaptive optics for free-space optical communications," in *Society of Photo-Optical Instrumentation Engineers (SPIE) Conference Series*, ser. Society of Photo-Optical Instrumentation Engineers (SPIE) Conference Series, vol. 7200, Feb. 2009.

[17] A. Montmerle Bonnefois, R. Biérent, M. Raybaut, A. Godard, S. Derelle, A. Durécu, V. Michau, M. Lefebvre, N. Védrenne, and M.-T. Velluet, "SCALPEL: a long range free-space optical communication system with adaptive optics in the MIR bandwidth," in *Society of Photo-Optical Instrumentation Engineers (SPIE) Conference Series*, ser. Society of Photo-Optical Instrumentation Engineers (SPIE) Conference Series, vol. 7828, Oct. 2010.

[18] M.-T. Velluet, G. Rousset, and T. Fusco, "Shack-Hartmann wavefront sensing errors induced by laser illumination," in *Society of Photo-Optical Instrumentation Engineers (SPIE) Conference Series*, ser. Society of Photo-Optical Instrumentation Engineers (SPIE) Conference Series, K. Stein and A. Kohnle, Eds., vol. 5981, Oct. 2005, pp. 188–196.

[19] N. Védrenne, A. Bonnefois Montmerle, C. Robert, V. Michau, J. Montri, and B. Fleury, "Cn2 profile measurement from Shack-Hartmann data: experimental validation and exploitation," in *Society of Photo-Optical Instrumentation Engineers (SPIE) Conference Series*, ser. Society of Photo-Optical Instrumentation Engineers (SPIE) Conference Series, vol. 7828, Oct. 2010.

[20] N. Muller, V. Michau, C. Robert, and G. Rousset, "Differential focal anisoplanatism in laser guide star wavefront sensing on extremely large telescopes," *Opt. Lett.*, vol. 36, no. 20, pp. 4071–4073, Oct 2011.

[21] N. Védrenne, V. Michau, C. Robert, and J.-M. Conan, "C_n^2 profile measurement from Shack-Hartmann data," *Opt. Lett.*, pp. 2659–2661, Sep. 2007.

[22] R.-E. Hufnagel, "Variations of atmospheric turbulence," in *Proc. of Topical Meeting on Optical Propagation through the Turbulence*, 1974.

[23] A. Monin and A. Obukhov, *Basic turbulent mixing laws in the atmospheric surface layer*. Trudy Geofiz. Inst. AN SSSR, 1954.

[24] J. C. Wyngaard, Y. Izumi, and S. A. Collins, Jr., "Behavior of the Refractive-Index -Structure Parameter near the Ground," *J. Opt. Soc. Am. A*, vol. 61, pp. 1646–+, Dec. 1971.

[25] J.-M. Conan, G. Rousset, and P.-Y. Madec, "Wave-front temporal spectra in high-resolution imaging through turbulence," *J. Opt. Soc. Am. A*, vol. 12, no. 12, pp. 1559–1570, Jul. 1995. [Online]. Available: mailto:conan@onera.fr

[26] M.-T. Velluet, V. Michau, T. Fusco, and J.-M. Conan, "Coherent illumination for wavefront sensing and imaging through turbulence," vol. 6708, pp. 670 808–670 808–9, 2007.

[27] M. Toyoshima, H. Takenaka, Y. Shoji, and Y. Takayama, "Frequency characteristics of atmospheric turbulence in space-to-ground laser links," in *Atmospheric Propagation VII*, vol. 7685. Proc. Soc. Photo-Opt. Instrum. Eng., 2010, pp. 76 850G–76 850G–12. [Online]. Available: + http://dx.doi.org/10.1117/12.850149

[28] D. Fried, "Optical resolution through a randomly inhomogeneous medium for very long and very short exposures," *J. Opt. Soc. Am. A*, vol. 56, pp. 1372–1379, 1966.

[29] V. Kornilov, A. A. Tokovinin, O. Vozyakova, A. Zaitsev, N. Shatsky, S. F. Potanin, and M. S. Sarazin, "MASS: a monitor of the vertical turbulence distribution," in *Adaptive Optical System Technologies II. Edited by Wizinowich, Peter L.; Bonaccini, Domenico. Proceedings of the SPIE, Volume 4839, pp. 837-845 (2003).*, P. L. Wizinowich and D. Bonaccini, Eds., Feb. 2003, pp. 837–845.

[30] A. Tokovinin, V. Kornilov, N. Shatsky, and O. Voziakova, "Restoration of turbulence profile from scintillation indices," *Mon. Not. R. Astr. Soc.*, vol. 343, pp. 891–899, Aug. 2003.

[31] J. Voyez, C. Robert, V. Michau, J. M. Conan, and T. Fusco, "Accurate measurement of Cn2 profile with Shack-Hartmann data," *ArXiv e-prints*, Jul. 2012.